

Novel isoquinolinium derivatives as inhibitors of acid corrosion

A.G. Berezhnaya,^{ID}* A.D. Zagrebaev, V.V. Chernyavina,^{ID} I.I. Krotkii
and V.V. Chernyavskaya

Southern Federal University, ul. Zorge 7, Rostov-on-Don, 344090 Russian Federation

*E-mail: Berezhnaya-aleksandra@mail.ru

Abstract

1-(4-Aminophenyl)-2-(9,10-dimethoxy-13-(7-nitrobenzo[*c*][1,2,5]oxadiazol-4-yl)-5,8-dihydro-6*H*-[1,3]dioxolo[4,5-*g*]isoquinolino[3,2-*a*]isoquinolin-8-yl)ethan-1-one (I), 2-(9,10-dimethoxy-13-(7-nitrobenzo[*c*][1,2,5]oxadiazol-4-yl)-5,8-dihydro-6*H*-[1,3]dioxolo[4,5-*g*]isoquinoline-3,2-*a*]isoquinolin-8-yl)-1-(4-methoxyphenyl)ethan-1-one (II) and 1-(4-chlorophenyl)-2-(9,10-dimethoxy-13-(7-nitrobenzo[*c*][1,2,5]oxadiazol-4-yl)-5,8-dihydro-6*H*-[1,3]dioxolo[4,5-*g*]isoquinolino[3,2-*a*]isoquinolin-8-yl)ethan-1-one (III) were studied as corrosion inhibitors of steel in 1 M hydrochloric acid at 20–80°C. The efficiency of the compounds was estimated by the gravimetric method, by recording polarization curves and by electrochemical impedance spectroscopy. Quantum-chemical calculations were carried out in the framework of the density functional theory (DFT). It was found that the best inhibitor, *i.e.*, compound III provides steel protection for 98 and 92% at temperatures of 25 and 80°C, respectively. The inhibitors hinder the corrosion process by changing the structure of the electrical double layer, blocking a fraction of the surface, and increasing the effective activation energy. The additives decrease the rates of both partial electrode reactions of the corrosion process. Calculations and optimization of inhibitor structures were carried out within the framework of functional theory. It was found that the best correlation is obtained for linear relationships: inhibition coefficient *vs.* X , where X is the energy of the highest occupied molecular orbital E_{HOMO} and the lowest unoccupied molecular orbital E_{LUMO} , electronegativity (χ) and the sum of electron densities on heteroatoms (ΣED).

Received: January 30, 2024. Published: February 11, 2024

doi: [10.17675/2305-6894-2024-13-1-15](https://doi.org/10.17675/2305-6894-2024-13-1-15)

Keywords: acid corrosion, inhibitor, isoquinoline derivatives, quantum-chemical calculations.

Introduction

Quinoline and isoquinoline derivatives have been studied as inhibitors of acid corrosion of steel [1–6]. The protective effect of quinoline derivatives depends on the nature of substituents. The protective effect of quinoline derivatives with grafted imidazoles at a concentration of 1 mM in 1 M hydrochloric acid amounts to 90.8 and 87.5% [2], while that of coumarin at a concentration of 0.5 mM is 85.5% [4]. The efficiency of berberine and dihydroberberine derivatives under similar conditions at a concentration of 0.3 mM was 93 and 92%, respectively [6]. The adsorption of the studied quinoline derivatives on steel

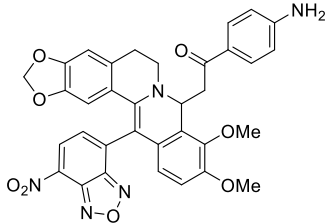
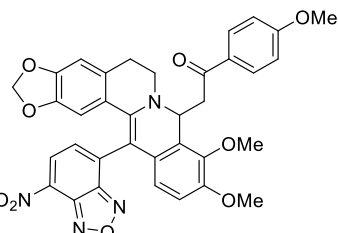
mostly occurs as physisorption and is described by the Langmuir isotherm [2, 3, 5]. Data from corrosion–electrochemical measurements were compared with calculated (density functional theory, DFT) characteristics of the molecules: energies of the highest occupied (E_{HOMO}) and lowest unoccupied (E_{LUMO}) molecular orbitals, their difference (ΔE), dipole moment (μ), electronegativity (χ), hardness (η), softness (σ), sum of effective charges on heteroatoms (ΣED), *etc.* It was found that the efficiency of some quinoline derivatives increased with an increase in E_{HOMO} and softness, a decrease in E_{LUMO} , dipole moment and hardness and is independent of electronegativity [1]. A correlation between the protective effect of inhibitors and calculated parameters of molecules was also noted by other researchers [2, 5, 6].

In this work, the protective effect of three novel isoquinoline derivatives on the corrosion of mild steel in hydrochloric acid was studied and their efficiency was compared with the calculated parameters of the molecules.

Experimental

The protective properties of the compounds (Tables 1, 2) in a concentration range of 10^{-5} – 10^{-4} mol/l toward the corrosion of low-carbon steel in 1 M hydrochloric acid solution were compared.

Table 1. Formula, name and some calculated characteristics of the organic compounds.

Formula and name of the compound	M , g/mol	E_{HOMO} , eV	E_{LUMO} , eV	μ , D
 1-(4-aminophenyl)-2-(9,10-dimethoxy-13-(7-nitrobenzo[<i>c</i>][1,2,5]oxadiazol-4-yl)-5,8-dihydro-6 <i>H</i> -[1,3]dioxolo[4,5- <i>g</i>]isoquinolino[3,2- <i>a</i>]isoquinolin-8-yl)ethan-1-one (I)	633	−4.611	−3.291	8.065
 2-(9,10-dimethoxy-13-(7-nitrobenzo[<i>c</i>][1,2,5]oxadiazol-4-yl)-5,8-dihydro-6 <i>H</i> -[1,3]dioxolo[4,5- <i>g</i>]isoquinolino[3,2- <i>a</i>]isoquinolin-8-yl)-1-(4-methoxyphenyl)ethan-1-one (II)	648	−4.643	−3.318	9.606

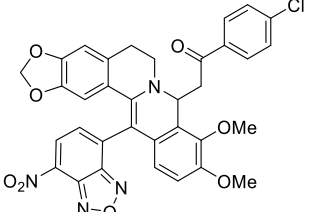
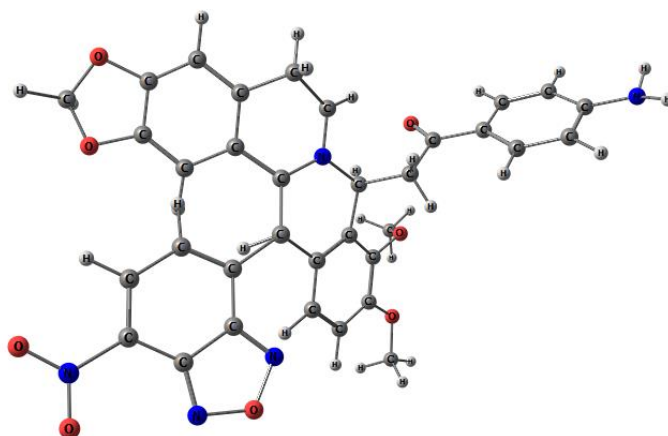
Formula and name of the compound	<i>M</i> , g/mol	<i>E</i> _{HOMO} , eV	<i>E</i> _{LUMO} , eV	μ , D
 <p>1-(4-chlorophenyl)-2-(9,10-dimethoxy-13-(7-nitrobenzo[<i>c</i>][1,2,5]oxadiazol-4-yl)-5,8-dihydro-6<i>H</i>-[1,3]dioxolo[4,5-<i>g</i>]isoquinolino[3,2-<i>a</i>]isoquinolin-8-yl)ethan-1-one (III)</p>	652.5	-4.744	-3.426	9.295

Table 2. Geometry of optimized molecules and some of their characteristics.

Compound I



Main Atomic Distances:

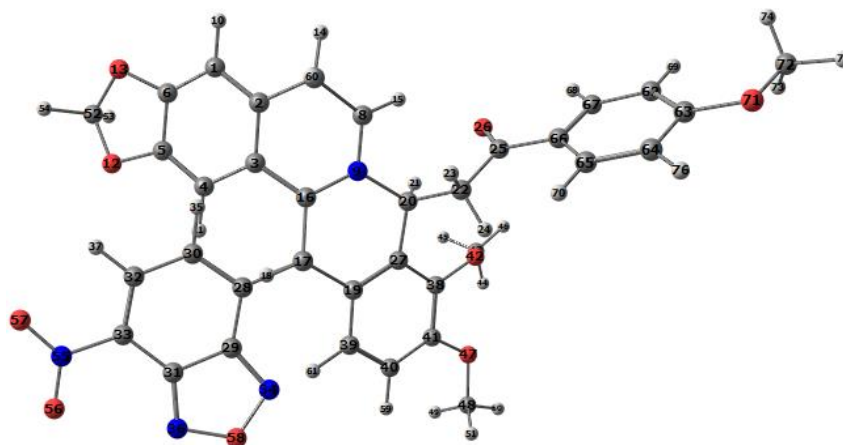
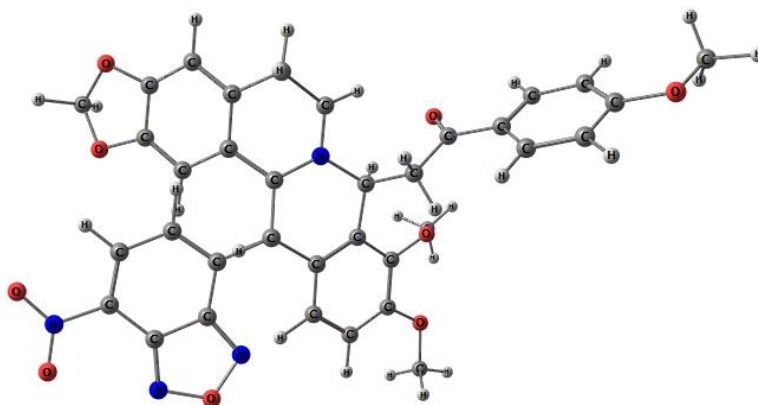
C–N (35–71) 1.383 Å
 N–H (71–72) 1.008 Å
 N–H (71–73) 1.008 Å
 N–O (64–65) 1.225 Å
 N–O (64–66) 1.231 Å
 C–N (42–64) 1.456 Å
 N–O (45–67) 1.371 Å
 N–O (43–67) 1.363 Å
 C–N (40–45) 1.317 Å
 C–N (38–43) 1.315 Å
 C–N (8–9) 1.332 Å
 C–N (16–9) 1.377 Å
 C–N (20–9) 1.508 Å

C–O (25–26) 1.224 Å
 C–O (6–13) 1.378 Å
 C–O (61–13) 1.430 Å
 C–O (61–12) 1.432 Å
 C–O (5–12) 1.379 Å
 C–O (47–51) 1.372 Å
 C–O (52–51) 1.435 Å
 C–O (50–56) 1.363 Å
 C–O (57–56) 1.421 Å

Main Atomic Charges:

9 N 1.061155
 12 O -0.123587
 13 O -0.124174
 26 O -0.057337
 43 N -0.730884
 45 N -0.301321
 51 O 0.120233
 56 O -0.085723
 64 N -0.338167
 65 O 0.055884
 66 O -0.017569
 67 O 0.736531
 71 N -0.591343

Compound II



Main Atomic Distances:

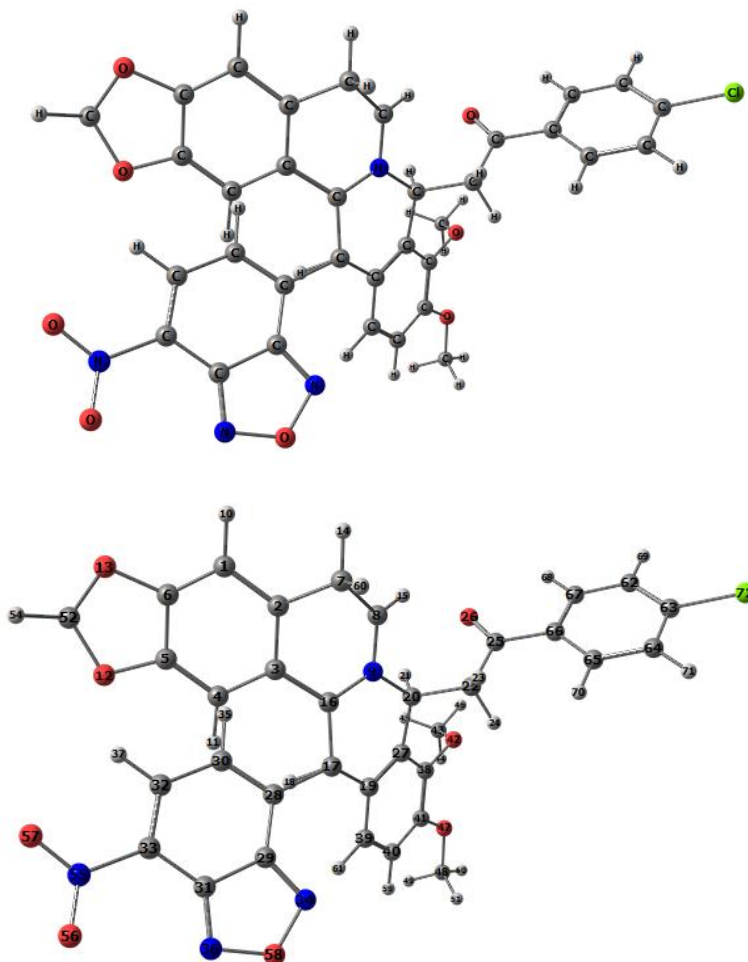
C–O (63–71) 1.357 Å
 C–O (72–71) 1.423 Å
 N–O (55–56) 1.225 Å
 N–O (55–57) 1.231 Å
 C–N (33–55) 1.457 Å
 N–O (36–58) 1.371 Å
 N–O (34–58) 1.363 Å
 C–N (31–36) 1.317 Å
 C–N (29–34) 1.315 Å
 C–N (8–9) 1.332 Å
 C–N (16–9) 1.376 Å
 C–N (20–9) 1.507 Å

C–O (25–26) 1.222 Å
 C–O (6–13) 1.377 Å
 C–O (52–13) 1.430 Å
 C–O (52–12) 1.432 Å
 C–O (5–12) 1.379 Å
 C–O (38–42) 1.373 Å
 C–O (43–42) 1.435 Å
 C–O (41–47) 1.363 Å
 C–O (48–47) 1.421 Å

Main Atomic Charges:

9 N 1.011002
 12 O –0.122852
 13 O –0.124320
 26 O –0.199018
 34 N –0.736138
 36 N –0.297883
 42 O 0.116966
 47 O –0.084825
 55 N –0.330338
 56 O 0.053570
 57 O –0.015475
 58 O 0.746578
 71 O –0.079014

Compound III



Main Atomic Distances:

C–Cl (63–72) 1.754 Å	C–O (25–26) 1.219 Å
N–O (55–56) 1.225 Å	C–O (6–13) 1.377 Å
N–O (55–57) 1.230 Å	C–O (52–13) 1.431 Å
C–N (33–55) 1.458 Å	C–O (52–12) 1.432 Å
	C–O (5–12) 1.378 Å
N–O (36–58) 1.370 Å	C–O (38–42) 1.373 Å
N–O (34–58) 1.364 Å	C–O (43–42) 1.435 Å
C–N (31–36) 1.317 Å	C–O (41–47) 1.363 Å
C–N (29–34) 1.315 Å	C–O (48–47) 1.422 Å
C–N (8–9) 1.334 Å	
C–N (16–9) 1.375 Å	
C–N (20–9) 1.506 Å	

Main Atomic Charges:

9 N 1.003453
12 O –0.123830
13 O –0.123415
26 O –0.205983
34 N –0.746816
36 N –0.276958
42 O 0.105731
47 O –0.084324
55 N –0.314783
56 O 0.044186
57 O –0.011502
58 O 0.734455
72 Cl 0.484652

Sample preparation and measurement methodology

Samples $0.2 \times 1 \text{ cm}^2$ in size for impedance measurements, $0.5 \times 1 \text{ cm}^2$ in size for polarization measurements, and $1 \times 2.5 \text{ cm}^2$ in size for corrosion measurements were cut from mild steel. The electrodes were cleaned with abrasive sandpaper, degreased in alcohol, washed with distilled water, and dried with filter paper. The working electrolyte was 1 M hydrochloric acid solution. Gravimetric measurements were carried out at temperatures of 25, 40, 60 and 80°C .

The corrosion rate K was calculated by formula (1):

$$K = \frac{\Delta m}{\tau \cdot S} \quad (1)$$

where Δm is the mass change (grams), τ is the experiment time (hours), and S is the sample area (m^2).

The efficiency of the additives was estimated by the inhibition coefficient γ (2) and the degree of protection Z (3):

$$\gamma = \frac{K_0}{K_i} \quad (2)$$

$$Z = \frac{(K_0 - K_i)}{K_0} \cdot 100\% \quad (3)$$

where K_0 and K_i are the corrosion rates in the pure acid and in the presence of an inhibitor, respectively.

Polarization measurements were carried out using an R-20X potentiostat-galvanostat (Elins Ltd., Russia) in a three-electrode thermostatically controlled cell at 25°C . A platinum counter electrode and a saturated silver chloride reference electrode were used. The potentials E are reported relative to the latter. Polarization curves were taken at a scan rate of 2 mV/s from the smaller $E = -0.7 \text{ V}$ to the larger $E = -0.3 \text{ V}$. Each curve was reproduced in triplicate, then the results were averaged.

Capacitance measurements were carried out on a Z-500 impedance meter (Elins LLC, Russia) in a two-electrode cell in the frequency range from 1 Hz to 300 kHz at the corrosion potential. A cylindrical platinum electrode served as the auxiliary electrode. The degree of coverage of the electrode surface was calculated by the formula:

$$\Theta = \frac{(S_0 - S_i)}{S_0} \quad (4)$$

where S_0 and S_i are the double electric layer (DEL) capacitances in the acid solution in the absence and in the presence of inhibitors, respectively.

Quantum-chemical calculations were performed in the framework of density functional theory (DFT) B3LYP/6-311+G(d) using Gaussian09 program [7]. Geometry optimization

was carried out without symmetry constraints. The DFT minima were characterized by the absence of imaginary frequencies of the calculated normal oscillations. The presented structures are obtained as a result of full optimization of all parameters and correspond to proven minimum points on the corresponding energy surfaces (PES). The electron density distribution was performed according to the Milliken scheme. The ChemCraft program [8] was used to visualize the results.

Results and Discussion

Isoquinoline derivatives have a branched π -system and comprise a few heteroatoms (N, O), including the carbonyl group (C=O). The adsorption of these compounds on steel surface can involve various moieties of the molecules as reaction centers. Both physical and chemical adsorption can take place. The compounds studied differ in the nature of the substituent in the *para* position of the phenyl radical, Table 1. The amino, methoxy and chloro groups differ in the ratio of inductive and mesomeric effects and act as electron-donor and electron-acceptor substituents. Incorporation of these groups into compounds leads to changes in the electron density (effective charge) on all heteroatoms and the bond lengths between the atoms, Table 2. This should affect their inhibitory effect on steel corrosion.

The dependence of the inhibition coefficient and degree of steel protection on the concentration of the compounds studied is presented in Table 3.

Table 3. Dependence of the inhibition coefficient and degree of protection on the concentration and nature of additives, $T=298$ K.

$C \cdot 10^3$, mol/L	Values of γ and $Z(\%)$ for the inhibitors					
	I		II		III	
	γ	$Z, \%$	γ	$Z, \%$	γ	$Z, \%$
0.010	5.9	83.1	11.0	90.9	15.3	93.5
0.025	6.6	84.8	13.2	92.4	20.4	95.1
0.050	6.7	85.1	15.6	93.6	27.5	96.4
0.075	9.3	89.2	16.2	93.8	40.7	97.5
0.100	10.9	90.8	18.0	94.4	48.8	98.0

As it can be seen from the data in Table 3, incorporation of an electron-acceptor substituent (chlorine) leads to an increase in the protective effect of the compound at all concentrations. The compounds studied can be as follows according to the growth in efficiency: $I < II < III$. With increasing temperature, the efficiency of compound III decreases, Figure 1.

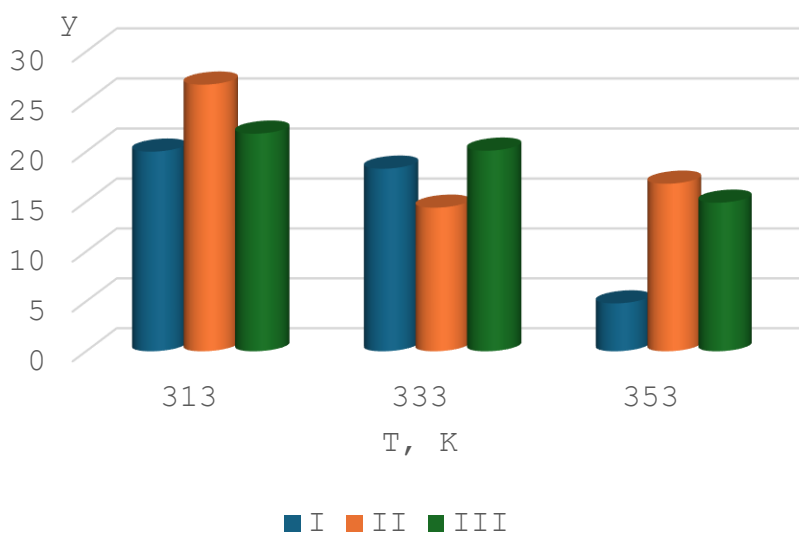


Figure 1. Dependence of the inhibition coefficient on temperature and nature of the compound at a concentration of $C=0.1$ mmol/L.

The inhibition coefficients of compounds I and II increase with increasing temperature compared to those at 298 K, reach maxima at $T=313$ K and then decrease, Figure 1, Table 3. Compounds II and III exhibit 93 and 92% efficiency at 353 K, respectively. All the inhibitors increase the effective activation energy (E_a) of the steel corrosion process. It was found that in the presence of compounds I, II and III in hydrochloric acid, E_a increased by 20, 12 and 8 kJ/mol compared to that in non-inhibited HCl.

It is known that, in addition to an increase in the effective activation energy, inhibitors reduce the corrosion rate by blocking a fraction of steel surface and changing the structure of the DEL. To estimate the contribution of these factors, it is necessary to consider the adsorption regularities of the compounds on steel surface. We analyzed the concentration dependence of the efficiency of compounds in the critical coordinates of the most common adsorption isotherms [9]. It was assumed that only the blocking or double-layer effect was realized. The highest correlation coefficients for the linear plots are obtained in the coordinates of the Langmuir isotherm under the assumption of purely blocking (I, II) and double-layer effects (III). The free adsorption energy of compounds (ΔG_{ads}) was calculated using Equation 5:

$$\Delta G_{ads} = -RT \ln(55.55B) \quad (5)$$

where R is the universal gas constant, T is the temperature, and B is the adsorption constant.

The ΔG_{ads} values for compounds I, II and III are -35.6 ; -32.9 and -38.8 kJ/mol. The ΔG_{ads} values indicate the presence of physical and chemical adsorption of compounds.

The Nyquist plots are shown in Figure 2.

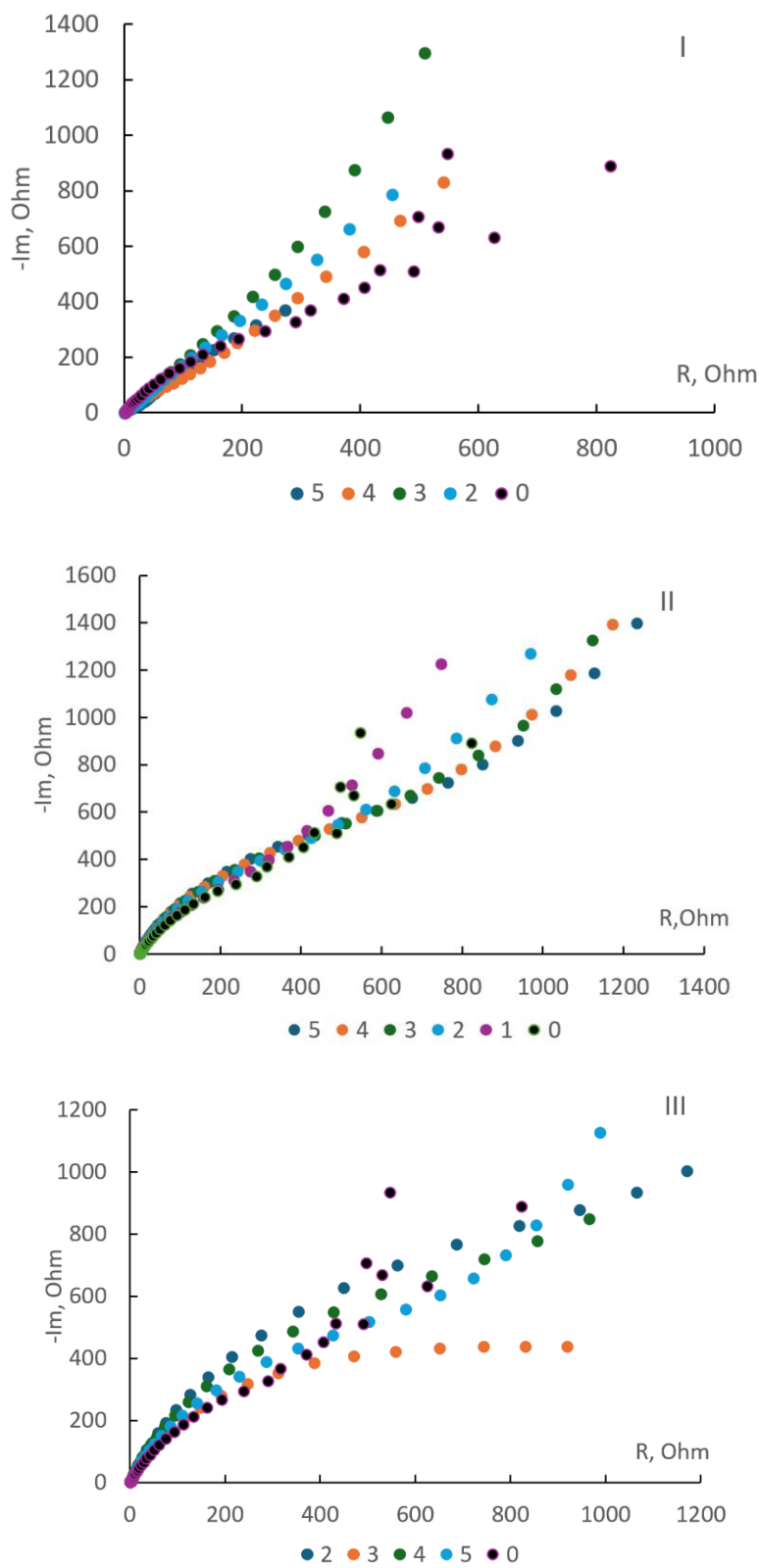


Figure 2. Nyquist plots of steel in 1 M HCl solution without inhibitors (0) and in the presence of inhibitors I, II, III at concentrations of 0.01 (1), 0.025 (2), 0.05 (3), 0.075 (4), and 0.1 mmol/L (5).

Upon addition of inhibitors and with an increase in their concentration, the Nyquist plots change in the entire frequency range. Using the selected equivalent circuits, the DEL capacitance was determined and the degrees of surface coverage with the inhibitors were calculated using formula (4), Table 4.

Table 4. Dependence of the degree of surface coverage on the concentration of inhibitors.

Inhibitor	Surface coverage θ (%) for C , mmol/L				
	0.01	0.025	0.05	0.075	0.1
I	22.6	24.8	18.8	24.8	55.7
II	40.6	60.9	63.5	68.3	69.2
III	–	36.2	33.8	29.4	73.6

The degree of surface coverage is smaller than the degree of protection at all concentrations, Tables 3, 4. This indicates a mixed mechanism of the protective action of these inhibitors.

According to the effect on the partial electrode reactions, the compounds studied belong to mixed type inhibitors. They inhibit the rates of both cathodic and anodic reactions and increase the corrosion potential, Figure 3.

The increase in the corrosion potential indicates that the inhibitors mainly affect steel dissolution. The compounds have an insignificant effect on the Tafel coefficient b_a , while they increase the polarizability of the cathodic reaction b_c with an increase in C , Table 5.

Table 5. Polarizabilities of the cathodic and anodic reactions in the presence of inhibitors in the solution (in 1 M HCl, $b_a=45$ mV, $b_c=120$ mV).

C , mmol/L	Parameter	0.01	0.025	0.05	0.075	0.1
I	b_a , mV	49	48	59	49	42
	b_c , mV	120	121	136	119	133
II	b_a , mV	48	52	43	44	34
	b_c , mV	140	162	168	168	183
III	b_a , mV	54	52	45	39	36
	b_c , mV	115	127	150	162	172

The protective effect of inhibitors (γ) was compared with the calculated characteristics of their molecules, such as: energy of the highest occupied E_{HOMO} and lowest unoccupied E_{LUMO} molecular orbitals, ΔE , electronegativity χ , dipole moment μ , hardness η , softness σ , and sum of electron densities on heteroatoms ΣED . Good correlation at all the studied

concentrations of the compounds is obtained for the relationships $\gamma-E_{\text{HOMO}}$, $\gamma-E_{\text{LUMO}}$, $\gamma-\Sigma ED$ and $\gamma-\chi$, Figure 4.

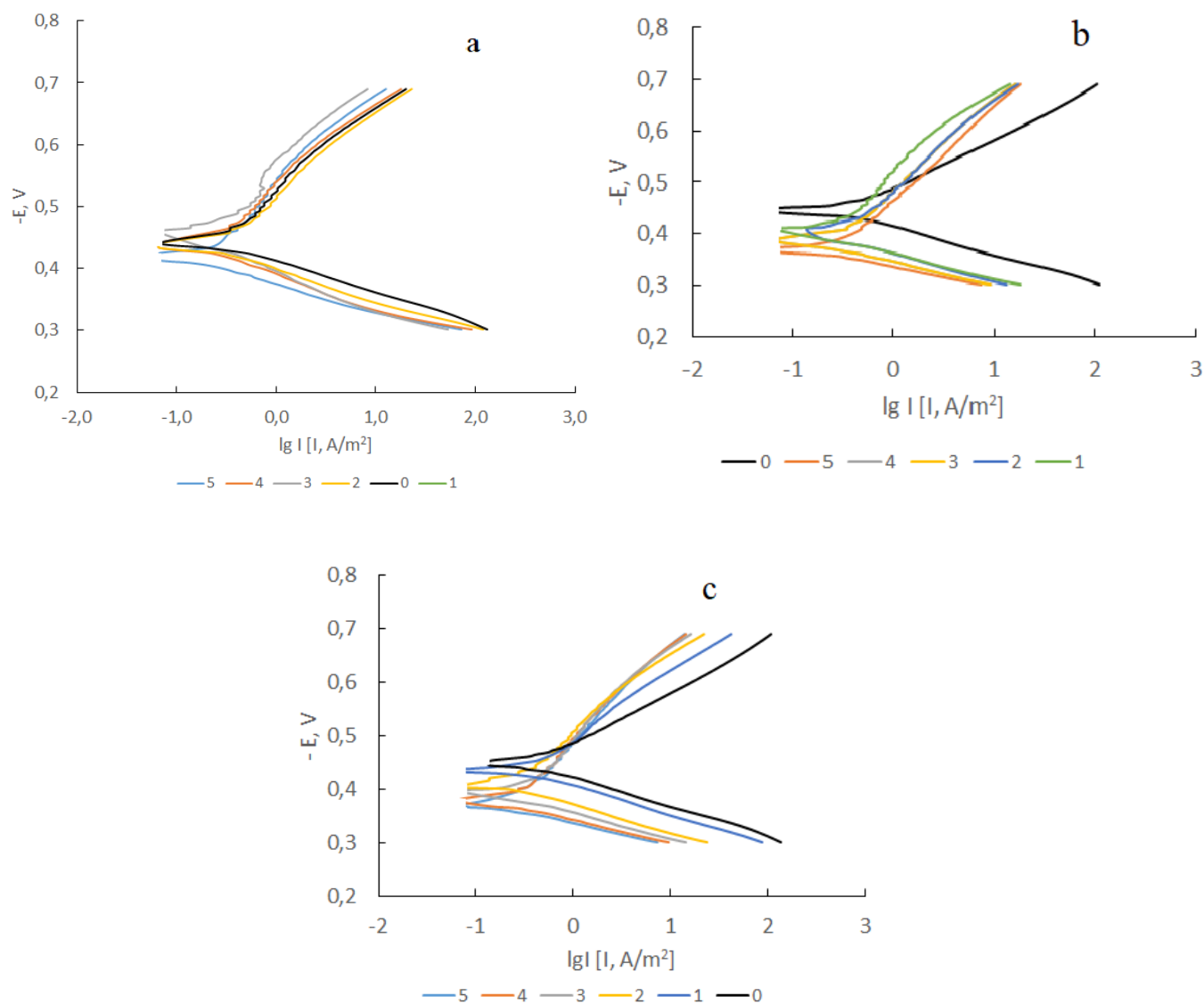


Figure 3. Polarization curves of steel in 1 M HCl solution without (0) and in the presence of inhibitors I (a), II (b), III (c) at concentrations of 0.01(1), 0.025 (2), 0.05(3), 0.075 (4), and 0.1 (5) mmol/L.

Thus, the efficiency of the compounds studied against corrosion of low-carbon steel in hydrochloric acid increases in the series $I < II < III$. The compounds are adsorbed on steel surface due to physical and chemical adsorption forces. The adsorption of the compounds is described by the Langmuir isotherm. The protective effect of the compounds is realized by an activation-blocking mechanism. The additives belong to mixed type inhibitors. The efficiency correlates well with the calculated parameters of the molecules.

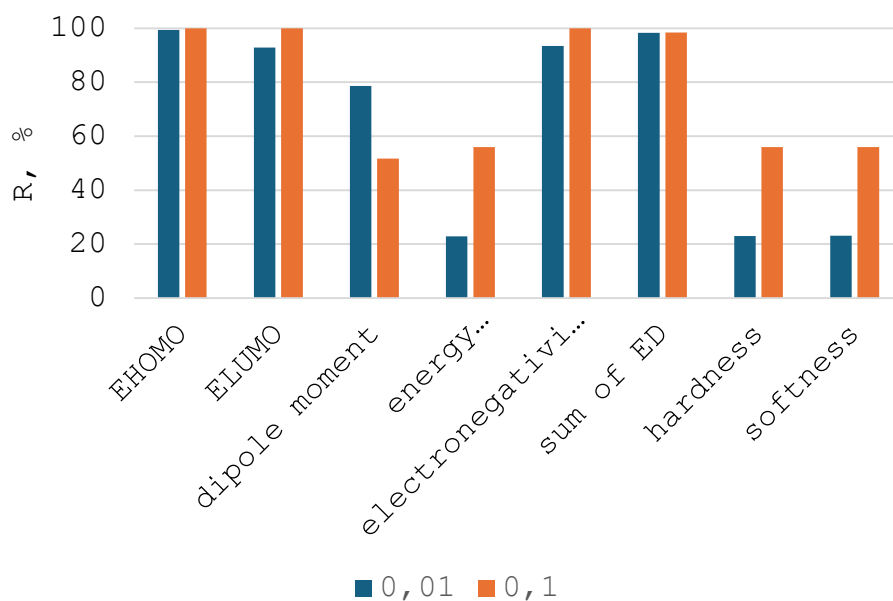


Figure 4. Correlation coefficients for the relationships $\gamma-X$, where $X=E_{\text{HOMO}}$, E_{LUMO} , μ , ΔE , χ , ΣED , η and σ at $C=0.01$ and 0.1 mmol/L.

References

1. E.A. Erazua and B.B. Adeleke, A Computational Study of Quinoline Derivatives as Corrosion Inhibitors for Mild Steel in Acidic Medium, *J. Appl. Sci. Environ. Manage.*, 2019, **23**, no. 10. doi: [10.4314/JASEM.V23I10.8](https://doi.org/10.4314/JASEM.V23I10.8)
2. A. Elbarki, Z. Amrani, T. Laabaissi, M. El Faydy, L. Adlani, A. Fatah, F. Benhiba, M. Rbaa, I. Warad, B. Lakhri, H. Zarrok, A. Bellaouchou, B. Dikici, H. Oudda and A. Zarrouk. The inhibitory effect of certain imidazole derivatives grafted on 8-hydroxyquinoline on carbon steel corrosion in acidic medium: experimental and computational approaches, *Int. J. Corros. Scale Inhib.*, 2023, **12**, no. 3, 1292–1320. doi: [10.17675/2305-6894-2023-12-3-27](https://doi.org/10.17675/2305-6894-2023-12-3-27)
3. W.N. Hussein, B.A. Hamza, M. Al-Shuraifi, R.A.H. Al-Uqaily and H.A. Kadhu. An Inhibitor (3-Methylisoquinoline) Prevents Mild Steel Corrosion in 1 M HCl Media, *Int. J. Adv. Multidisc. Res. Stud.*, 2022, **2**, no. 4, 22–26.
4. Y.K. Al-Majedy, H.H. Ibraheem, A.A. Issa and A. Alamiery. Exploring chromone derivatives as environmentally friendly corrosion inhibitors for mild steel in acidic environments: A comprehensive experimental and DFT study, *Int. J. Corros. Scale Inhib.*, 2023, **12**, no. 3, 1028–1051. doi: [10.17675/2305-6894-2023-12-3-14](https://doi.org/10.17675/2305-6894-2023-12-3-14)
5. M.E. Said, H. Allal, B. Mezhoud, M. Bouchouit, A. Chibani and A. Bouraiou, Experimental and theoretical evaluation of (*iso*)quinolinium bromide derivatives as corrosion inhibitors of steel E24 in 0.5 M H_2SO_4 solution, *Int. J. Corros. Scale Inhib.*, 2023, **12**, no. 2, 679–695 doi: [10.17675/2305-6894-2023-12-2-16](https://doi.org/10.17675/2305-6894-2023-12-2-16)

-
6. A.G. Berezhnaya, V.V. Chernyavina and I.I. Krotkii, Pyriliium perchlorate and berberine derivatives as inhibitors of hydrochloric acid corrosion of steel, *Korroz.: Mater., Zashch.*, 2022, no. 2, 37–42 (in Russian). doi: [10.31044/1813-7016-2022-0-2-37-42](https://doi.org/10.31044/1813-7016-2022-0-2-37-42)
 7. M.J. Frisch, G.W. Trucks, H.B. Schlegel, G.E. Scuseria, M.A. Robb, J.R. Cheeseman, G. Scalmani, V. Barone, B. Mennucci, G.A. Petersson, H. Nakatsuji, M. Caricato, X. Li, H.P. Hratchian, A.F. Izmaylov, J. Bloino, G. Zheng, J.L. Sonnenberg, M. Hada, M. Ehara, K. Toyota, R. Fukuda, J. Hasegawa, M. Ishida, T. Nakajima, Y. Honda, O. Kitao, H. Nakai, T. Vreven, J.A. Montgomery, Jr., J.E. Peralta, F. Ogliaro, M. Bearpark, J.J. Heyd, E. Brothers, K.N. Kudin, V.N. Staroverov, R. Kobayashi, J. Normand, K. Raghavachari, A. Rendell, J.C. Burant, S.S. Iyengar, J. Tomasi, M. Cossi, N. Rega, J.M. Millam, M. Klene, J.E. Knox, J.B. Cross, V. Bakken, C. Adamo, J. Jaramillo, R. Gomperts, R.E. Stratmann, O. Yazyev, A.J. Austin, R. Cammi, C. Pomelli, J.W. Ochterski, R.L. Martin, K. Morokuma, V.G. Zakrzewski, G.A. Voth, P. Salvador, J.J. Dannenberg, S. Dapprich, A.D. Daniels, Ö. Farkas, J.B. Foresman, J.V. Ortiz, J. Cioslowski and D.J. Fox, *Gaussian 09, Revision A.02*, Gaussian, Inc., Wallingford CT, 2009.
 8. <https://www.chemcraftprog.com>
 9. A.G. Berezhnaya, I.I. Krotky and V.V. Chernyavina, Protective effect of imidazobenzimidazoline dihydrochlorides against the acid corrosion of steel, *Int. J. Corros. Scale Inhib.*, 2023, 12, no. 4, 2418–2430. doi: [10.17675/2305-6894-2023-12-4-51](https://doi.org/10.17675/2305-6894-2023-12-4-51)

